Physical Communication 26 (2018) 106–115

Contents lists available at ScienceDirect

Physical Communication

journal homepage: www.elsevier.com/locate/phycom

Review article

Impact of partial phase decorrelation on the performance of pilot-assisted millimeter-wave RoF-OFDM systems

David Zabala-Blanco [a,*], Gabriel Campuzano [a], Ivan Aldaya [b], Gerardo Castañón [a], César Vargas-Rosales [a]

[a] Department of Electrical and Computer Engineering, Tecnológico de Monterrey, 64849 Monterrey, Mexico
[b] State University of Sao Paulo, 505 Sao Paulo, Brazil

ARTICLE INFO

Article history:
Received 14 July 2017
Received in revised form 7 November 2017
Accepted 6 December 2017
Available online 11 December 2017

Keywords:
Orthogonal frequency division multiplexing
Partially phase-correlated fields
Pilot-assisted phase-noise estimation
Radio over fiber systems

ABSTRACT

It is well known that in radio over fiber (RoF) systems, the transmission performance of orthogonal frequency-division multiplexing (OFDM) is highly sensitive to phase noise. In these systems, the radio frequency (RF) signal is generated by beating a reference and a modulated signal at the base station and, therefore, the phase noise of the RF signal depends on the phase noise of both reference and modulated signals as well as on the correlation between them. In many RoF systems, the reference and modulated signals come from the same optical source and, consequently, they are affected by the same phase noise, i.e., perfect correlation. Unfortunately, chromatic dispersion of fiber progressively decorrelates the phase noise affecting both signals. This impairment is especial detrimental in RoF systems operating at millimeter waves, limiting the maximum achievable range. On the other hand, pilot-aided equalization has proven its potential to combat the impact of phase noise in OFDM signals. However, the complex interrelation between phase noise induced by partial decorrelation and pilot-aided equalization is still uncertain. In this paper, we present extensive simulation and theoretical results to assess the optical signal to noise penalty and range limitation caused by partial field decorrelation. We discovered three performance regimes in terms of the correlation degree. This finding was explained by both the profile of the power spectral density and the subcarrier phase noise. Whereas the former is a qualitative result, the latter allows to quantify the phase noise for an OFDM signal with partial decorrelation and phase noise mitigation. Our results revealed that the appearance of a third operating regime is due to pilot-assisted equalization. Finally, we found the range of RoF-OFDM systems for perfectly correlated fields at the transmitter.

Contents

* Corresponding author.
E-mail address: A00813590@itesm.mx (D. Zabala-Blanco).

https://doi.org/10.1016/j.phycom.2017.12.002
1874-4907/

1. Introduction

The exploitation of millimeter-waves (mm-waves) has been extensively proposed to overcome the current traffic saturation at frequencies below 5 GHz in multiple wireless networks [1]. Projections predict a 10,000-fold increase of wireless traffic demand by 2025 with respect to 2013 [2]. Some of the popular mm-wave bands contemplated are the V-band (57–64 GHz) and E-band (71–76 GHz and 81–86 GHz). Firstly, the upcoming standard IEEE 802.11ad (WiGig) has adopted the V-band due to the broad unlicensed bandwidth of 7 GHz and to the high atmospheric attenuation, which leads to a higher degree of cell confinement [3]. Secondly, the E-band has been identified for 5*th* generation cellular networks (5G) due to the lower losses, the high bandwidth assigned per channel (5 GHz), and the reduced latency over large distances [4]. Moreover, the FCC has been recently considered the assignment of 102–109.5 GHz band for fixed mm-wave applications, but service rules have not yet been established [5]. It is clear then that mm-waves will play an important role in future high capacity wireless communications.

Although there is high bandwidth available at mm-waves, network design poses the challenge of feeding numerous base stations while keeping their cost as low as possible [6]. Radio over fiber (RoF) systems have been consistently proposed to solve this issue [1,7]. They are composed of a central station, base stations, and mobile terminals [8], Fig. 1 depicts a simple RoF system architecture. The output of the central station can be seen as the combination of two optical tones (the reference and modulated signals), and is generated by employing some optical up-conversion technique, such as mode-locked lasers, gain-switched laser, optical two-tone or multi-tone generation employing external optical modulators, gain-switched laser, among others [6,9–11]. In consequence, the mm-wave signal is given by direct photo-detection at the base stations [1]. The frequency difference between these tones must match, of course, the desired mm-wave frequency. RoF systems amalgamate optical fiber and wireless communications exploiting benefits of each link: low fiber attenuation, large fiber bandwidth, improved wireless coverage, and low transmit power, for instance [12]. Notice, however, that these systems require high-speed optical components for optical up-conversion at the central station and for photodetection at the base stations. Their impairments, such as laser phase noise, relative intensity noise, shot noise, and thermal noise affect the system performance [8]. Additionally, fiber chromatic dispersion limits the overall bandwidth-distance product [1,6].

Orthogonal frequency-division multiplexing (OFDM) is the most promising modulation format for RoF systems owing to its robustness against inter-symbol interference caused by both fiber dispersion in optical fibers and multipath effects in wireless channels [13]. The adoption of OFDM is based not only on this advantage but also on the high spectral efficiency and the flexibility for implementing medium access schemes [14]. As a result, OFDM has been adopted by popular standards, for example, digital subscriber line (DSL), digital video broadcasting (DVB), wireless fidelity (WiFi), and long-term evolution (LTE) [15], and has been proposed for future communication systems including next generation passive optical networks (NG-PON), WiGig, and 5G [14,16]. For OFDM to perform adequately, the orthogonality between its subcarriers must be kept during the transmission, propagation, and detection of a single OFDM symbol. Unfortunately, two main physical impairments known as oscillator frequency detuning and phase noise, cause loss of orthogonality and consequently degradation of system performance [15]. The local oscillator detuning from the received carrier frequency is easily corrected by including a synchronization preamble in every frame [17,18]. Phase noise, at least for low radio frequency (RF) applications, is typically not a concern because oscillators based on CMOS technology easily meet phase error specifications [19]. The effect of phase noise on OFDM performance has nevertheless been studied in the RF domain [20–22] revealing that it causes subcarrier phase rotation, denominated common phase error (CPE), and inter-carrier interference (ICI). While ICI is difficult to reduce, CPE may be mitigated by pilot-based channel estimation [23,24], which, by the way, is systematically included in most OFDM implementations for wireless channel equalization [25]. For instance, Armada et al. [26] experimentally demonstrated this correction scheme to combat not only a frequency-selective channel but also the phase noise in a modem for digital television.

Phase noise is especially relevant in optical fiber communications because it arises from semiconductor lasers with a broad linewidth [15]. Previous studies [27–29] on the impact of phase noise for optical OFDM transmissions can be classified by the type of detection. For coherent detection, laser linewidth is a critical parameter since the phase noise of the photocurrent is produced by the beating of the transmitter laser field and local oscillator, which are usually uncorrelated [27]. Consequently, numerous proposals to diminish the phase noise in different scenarios, such as PON and long-haul, have been demonstrated in [30–35]. Among the phase noise compensators reported, they highlighted pilot-aided and RF-pilot mitigation. In pilot-aided mitigation, several pilot tones are embedded within the OFDM signal, while in RF-pilot mitigation, a dc tone is inserted leaving an RF guard band between it and the OFDM signal. While the former only compensates CPE, the latter reduces both CPE and ICI [32]. The RF-pilot mitigation thus enables the use of noisier lasers at the expense of an increase of system complexity. It is evident, though, that these results are exclusively valid for phase-uncorrelated fields arising usually from beating the optical signal with an unsynchronized local oscillator.

In OFDM-based RoF systems, the resulting phase noise comes not only from laser phase noise but also from fiber dispersion, causing CPE and ICI again [28,29]. Although these authors define a phase rotation term that is slightly different for each subcarrier, the difference between the dispersion-induced phase noise of the first and last subcarrier may be considered negligible for practical systems. In particular, for these systems, the effect of partially correlated fields on the system performance has been briefly analyzed in [36,37]. They studied how the system is affected by the amount of phase-correlation between the combined optical tones presenting results for a few fiber lengths with and without time delay precompensation in order to diminish the phase noise. We therefore believe that a thorough study of the bit error rate (BER) is necessary because the received OFDM signal has usually partially decorrelated subcarriers due to fiber dispersion.

In this paper, we assess the impact of phase-correlation between the fields in RoF-OFDM performance. Our results can be applied to OFDM-based RoF systems employing most famous optical up-conversion techniques, such as externally modulated laser, multimode light sources, and heterodyning two lasers. Even if the optical tones are perfectly phase-correlated at the central station, the distribution through a length of fiber will partially or completely decorrelate them. First of all, we discovered three performance regimes of the BER as the decorrelation degree between the fields was varied through the time delay parameter. We then performed numerical simulations to explain this behavior since the previous theoretical results only predicted the existence of two regimes. By introducing the subcarrier phase noise and the equivalent laser linewidth after pilot-assisted equalization, we were able to theoretically describe the three operating regimes. This result was further verified by observing the power spectral density (PSD) profile of the received OFDM signal together with the effectiveness of the phase noise compensator. After that we studied the laser phase noise and additive white Gaussian noise

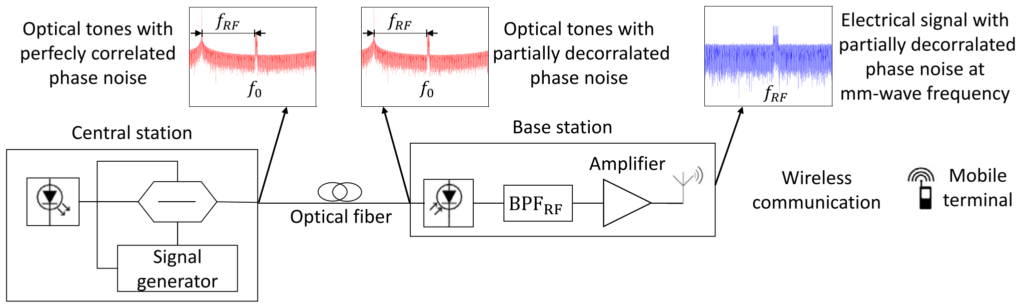

Fig. 1. Simple RoF system architecture. BPF$_{RF}$: band pass filter centered at RF.

(AWGN) effects. As the laser linewidth increases, its coherence time decreases approaching the OFDM symbol period and only two performance regimes may be identified. Regarding AWGN, its influence on the BER is negligible compared to laser phase noise for a signal-to-noise-ratio (SNR) above 30 dB. To conclude, we found the transmission distance for RoF-OFDM systems with perfectly phase-correlated at the central station. On these systems, the transmission distance is loss-limited for narrow laser linewidths and dispersion-limited for broad laser linewidths. Nevertheless, the dispersion limit could be relaxed by employing a particular time delay precompensation at the central station or a dedicated phase noise mitigation method in the OFDM modem.

This paper is organized as follows: Section 2 describes the simulation setup including the RoF system and OFDM modem. The methods to determine the BER, error vector magnitude (EVM), and subcarrier phase noise, are also described here. In Section 3, the simulated and theoretical results are presented, highlighting the impact of the degree of phase-decorrelation between the beating fields on system performance. The transmission distance for a variety of RoF-OFDM systems is then discussed in Section 4, and finally, conclusions are presented in Section 5.

2. System model and methodology

2.1. General scheme of a radio over fiber system

Based on [38], Fig. 2(a) shows the general simulation setup of a RoF system. The field emitted far above threshold by a single-frequency semiconductor laser can be represented as a quasi-monochromatic amplitude-stabilized field subject to phase fluctuations [39]:

$$E(t) = E_0 \ \exp\{j[2\pi f_0 t + \phi(t)]\}, \tag{1}$$

where $E_0 = \sqrt{0.5}$ V/m is the field amplitude, f_0 is the central frequency, and $\phi(t)$ is the phase noise, which is modeled as a Wiener process with zero mean and variance $2\pi\Delta\nu/f_s$ [40]. $\Delta\nu$, called laser linewidth, is the full width at half maximum of the semiconductor laser and $f_s = 100$ GHz is the sampling rate that we adopt to develop our numerical model. The laser output is then split into two fields, the reference field, which is frequency-shifted and delayed, and the modulated field. The reference field is given by:

$$E_{ref}(t) = E(t+\tau_0) \ \exp[-j2\pi f_{RF}(t+\tau_0)], \tag{2}$$

where τ_0 is the time delay, which models the phase-decorrelation degree between the reference and modulated fields, and f_{RF} is the desired RF. At the same time, τ_0 can model the effect of fiber dispersion since the separation between OFDM subcarriers is much less than f_{RF} throughout the paper [41]. For a time delay equal to 0 s, the fields are perfectly phase-correlated, for small time delays, there is partial phase-decorrelation between the fields, and for time delays greater than $1/\Delta\nu$, the fields become completely phase-decorrelated [38,42]. $1/\Delta\nu = T_c$, called coherence time, is the time over which the laser phase noise remains relatively stable [43]. Meanwhile, the analytic signal associated to the modulated field can be written as:

$$E_s(t) = E(t)\, s(t), \tag{3}$$

where $s(t)$ is the complex-valued OFDM signal. We limit our study to the case of linear field modulation in the absence of the optical carrier in order to focus the impact of the amount of phase-correlation between the beating optical tones. Afterwards, the reference and modulated fields are combined resulting in:

$$E_T(t) = E_{ref}(t) + E_s(t). \tag{4}$$

The total field, $E_T(t)$, is then down-converted to the electrical domain through a square-law detector with AWGN to account for shot and thermal noises [43]. The photogenerated current, which is composed of low-frequency components and the band-pass component centered at RF, is then expressed as:

$$\tilde{i}_{pd}(t) = R\, |E_T(t)|^2 + \tilde{n}(t), \tag{5}$$

with $R = 1$ A/W and $\tilde{n}(t)$ representing the photodetector responsivity and AWGN, respectively. By inserting the total field in Eq. (5), the photogenerated current can be represented as:

$$\tilde{i}_{pd}(t) = 2\, R\, E_0^2\, Re\big\{s(t)\ \exp\{j[2\pi f_{RF} t + \phi_0 + \Delta\phi(t,\tau_0)]\}\big\} + R\, E_0^2\, (1 + |s(t)|^2) + \tilde{n}(t), \tag{6}$$

where $\phi_0 = 2\pi(f_{RF} - f_0)\tau_0$ is a time-invariant phase shift and $\Delta\phi(t,\tau_0) = \phi(t) - \phi(t+\tau_0)$ is the random phase change induced by the decorrelation between the fields. For simplicity, the constant phase shift is here suppressed thanks to the pilot-assisted phase-noise estimation. The photogenerated current is then filtered by an ideal band pass filter centered at RF to remove the low-frequency components and converted to an analytic signal using the Hilbert transform, hence resulting in:

$$i_{pd}(t) = 2\, R\, E_0^2\, s(t)\ \exp\{j[2\pi f_{RF} t + \Delta\phi(t,\tau_0)]\} + n(t), \tag{7}$$

where $n(t)$ is the analytic signal associated to the filtered AWGN. Finally, the complex-valued input to the OFDM demodulator after down-conversion, acquires the form of:

$$r(t) = 2\, R\, E_0^2\, s(t)\ \exp[j\Delta\phi(t,\tau_0)] + n'(t), \tag{8}$$

where $n'(t) = n(t)\ \exp(-j2\pi f_{RF} t)$. The received OFDM signal is therefore corrupted by phase noise as well as by AWGN that induces both amplitude noise and phase noise.

2.2. OFDM stages

Fig. 2(b) shows the simulation setup of the OFDM modem. At the OFDM modulator, the input serial data bits are first converted

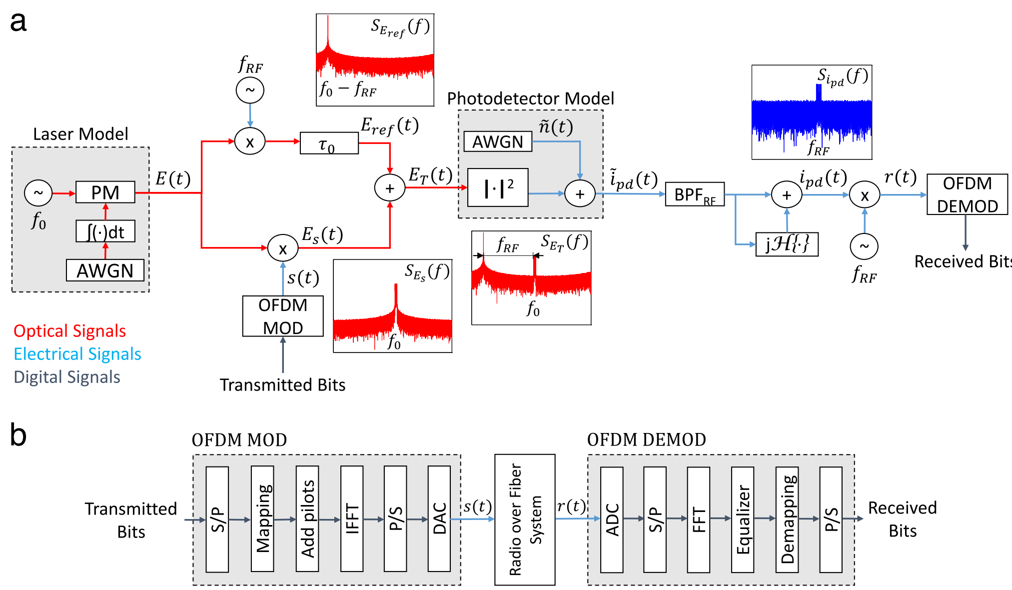

Fig. 2. (a) Block diagram of the simulated RoF system. AWGN: additive white Gaussian noise, PM: phase modulator, τ_0: time delay, OFDM MOD: OFDM modulator, BPF$_{RF}$: band pass filter centered at RF, and OFDM DEMOD: OFDM demodulator. (b) OFDM modem. S/P: serial-to-parallel, IFFT: inverse fast Fourier transform, P/S: parallel-to-serial, DAC: digital-to-analog converter, ADC: analog-to-digital converter, and FFT: fast Fourier transform.

into 56 parallel data pipes that are mapped to a 16 quadrature amplitude modulation (QAM) constellation using Gray code. 8 pilots are next added uniformly along the data streams before feeding to the inverse fast Fourier transform (IFFT) module. Although in [44], it is proven that the best performance is obtained when using non-uniformly spaced pilots, our intent is to study system degradation as the heterodyning optical tones become decorrelated. Pilots are usually employed to estimate the wireless channel, but here, we use them to combat CPE caused by the phase noise. The data stream is serialized and oversampled with a minimum factor of 35 to mimic a digital-to-analog converter. At the receiver, the OFDM signal is first sampled at the ratio between 56+8=64 subcarriers and the OFDM symbol period, T_s, in order to emulate an analog-to-digital converter. This output is then parallelized and demodulated by performing the fast Fourier transform (FFT). After that the signal is equalized by linearly interpolating the data from the 8 demodulated pilots. Hard-decision demapping results in the parallel bit streams, which are finally converted to serial. The equalization employs the linear interpolation between pilots because it presents low complexity while keeping acceptable performance [45].

2.3. Theoretical system performance without phase noise compensation

A well known approximation of the BER as a function of the root mean square EVM can be found in [46], where perfect carrier recovery for a Gaussian noise channel is assumed:

$$BER \approx \frac{2(1-\frac{1}{L})}{\log_2 L} \mathrm{Q}\left\{\left[\frac{3\log_2 L}{L(L^2-1)EVM^2}\right]^{1/2}\right\}, \tag{9}$$

with L and Q[·] representing the number of levels in each dimension of the M-ary subcarrier modulation format and the Gaussian co-error function, respectively. $EVM^2 = 1/(2 \times SNR)$ further relates the EVM to the SNR. However, in the presence of phase noise induced by both the decorrelation between the fields and the laser phase noise, this acquires the form of [47]:

$$EVM^2 = \frac{1}{2 \times SNR} + 1 - \exp\left(-\frac{\sigma^2}{2}\right), \tag{10}$$

where σ^2 is the variance of the random phase change induced by decorrelation between the combined optical tones given by [38,42]:

$$\sigma^2 = 4\pi\,\Delta\nu\,\tau_0. \tag{11}$$

And as mentioned at Section 2.1, $\Delta\nu$ is the laser linewidth and τ_0 is the time delay parameter. Hence, without phase noise mitigation, it is possible to theoretically know how system performance is affected by the amount of phase-correlation between the fields.

2.4. Performance metrics

Different performance metrics have been employed along the paper, such as the BER, EVM, and subcarrier phase noise. The error counting method is first selected for its simplicity in assessing the BER, but for low BERs a high number of bits needs to be simulated. As a rule of thumb, the simulation of $b = 100/(m \times BER)$ bits is required to obtain a confidence level of 99% where m is the number of runs [48,49]. In each simulation, we performed 100 runs of 104 832 pseudo-random bits allowing measurements of a BER in the order of 10^{-5}. In regards to the forward error correction (FEC) limit, we adopt a BER threshold equal to 10^{-3} that would allow reduction to 10^{-12} using modern FEC architectures [50].

Afterwards, the EVM is extensively applied as a performance measure of communication systems, specially in those using multi-level modulation formats [51]. For OFDM signals, the average EVM is defined as [52]:

$$EVM = \frac{1}{m}\sum_{i=0}^{m-1}\left(\frac{\sum_{k=0}^{N_s-1}\sum_{l=0}^{N_{sc}-1}|s_{lki}-r_{lki}|^2}{N_s\,N_{sc}\,P_0}\right)^{1/2}, \tag{12}$$

where N_s is the number of OFDM symbols, N_{sc} is the number of subcarriers, and P_0 is the average power of the constellation. Meanwhile, s_{lki} and r_{lki} are the transmitted and received symbol constellation of the ith run, kth OFDM symbol of the run, and lth subcarrier of the OFDM symbol, respectively. Notice that since the phase noise causes both CPE and ICI and that the former may be compensated through pilot-assisted phase-noise correction, the EVM mainly measures ICI. We follow the BER's rule of thumb to obtain EVMs with confidence level of 99%, too.

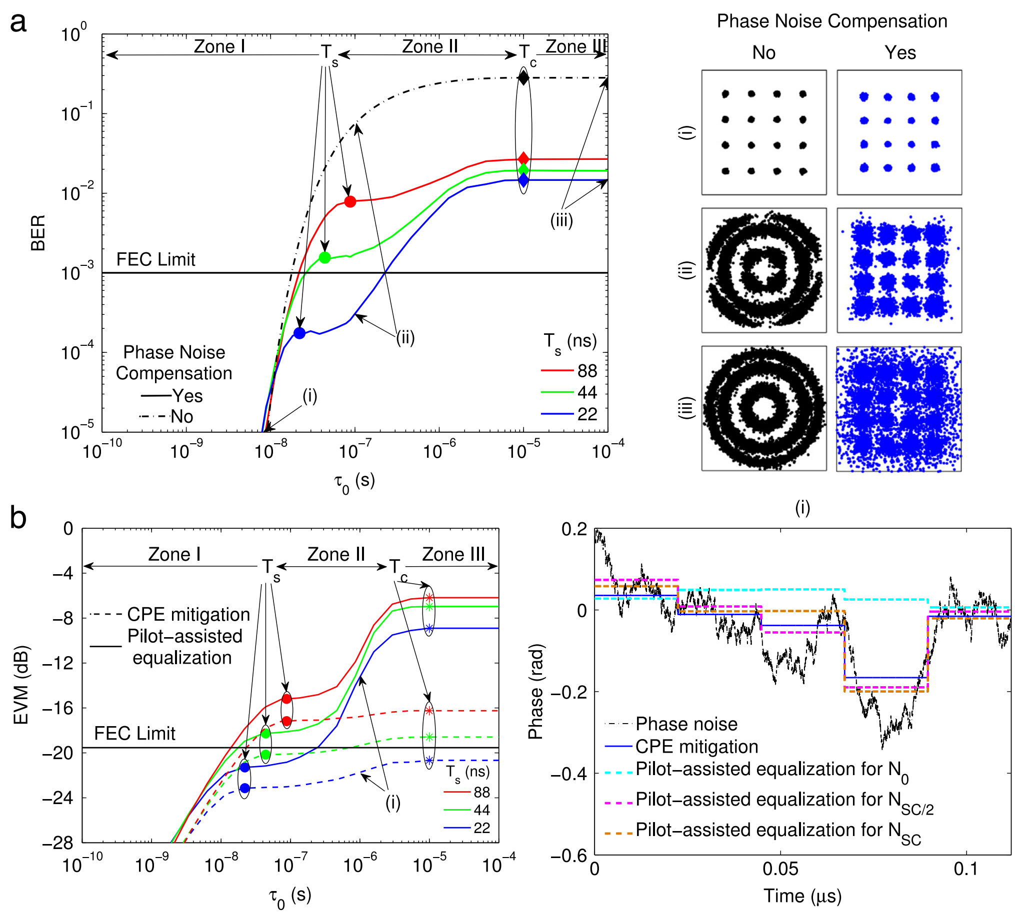

Fig. 3. (a) BER in terms of the time delay in the absence (dash–dot curve) and in the presence (solid curves) of pilot-assisted equalization. For solid curves, the OFDM symbol period is the parameter. (a.i-iii) Constellations without (black points) and with (blue points) phase noise reduction in each zone. (b) EVM as a function of the time delay utilizing pilot-assisted phase-noise estimation (solid curves) and CPE reduction (dashed curves) with the OFDM symbol period as parameter. (b.i) Estimated phase noises according to the employed phase noise compensator along some OFDM symbol periods. The considered laser linewidth was 100 kHz and AWGN was not taken into account. (For interpretation of the references to color in this figure legend, the reader is referred to the web version of this article.)

And finally for our system, a new way to measure the phase noise as the optical tones become decorrelated is introduced. There are different ways to quantify phase noise [53]. The most common one for single-carrier systems is denominated single sideband phase noise, which is defined as the ratio of the PSD measured at an offset frequency from the carrier to its power [54]. To characterize the phase-noise strength in OFDM systems, the relative phase noise bandwidth is typically used [55]. It is simply given by the ratio between the 3-dB linewidth of the oscillator and the subcarrier spacing. Unfortunately, this definition cannot characterize an optically generated carrier produced by partially phase-decorrelated fields. In fact, a carrier with perfect phase-correlation or partial phase-decorrelation would have the same relative phase noise. We therefore introduce the subcarrier phase noise adopting the definition used in single carrier systems: the ratio between the PSD at an offset frequency from the subcarrier and the power in the subcarrier bandwidth. The offset frequency, which must be less than the laser linewidth in order to obtain monotonically increasing results, was set to 10 kHz. For an OFDM signal with phase noise, the subcarrier phase noise is exposed in the Appendix.

3. Results

3.1. System performance

The impact of phase-decorrelation between the mixed optical tones on the system performance is first studied. We chose a laser linewidth of 100 kHz to model an external cavity laser whose coherence time is 10 μs. AWGN is not considered for the moment. Solid curves in Fig. 3(a) depict the BER vs. time delay with phase noise mitigation for the next OFDM symbol periods: 88, 44, and 22 ns. The time delay degrades the system performance following a behavior as is described next. Obviously, with perfect phase-correlation between the fields, *i.e.* $\tau_0 = 0$ s, the BER is equal to 0 because it corresponds to a pure RF carrier. When the fields are partially decorrelated, *i.e.* $\tau_0 < T_c$, two BER regimes are distinguished, labeled zone I and II. The first zone is limited to time delays less than the OFDM symbol period, *i.e.* $\tau_0 < T_s$, where the BER rapidly deteriorates. Meanwhile, the BER slowly deteriorates in the second zone, for time delays greater than the OFDM symbol period and less than the coherence time, *i.e.* $T_s < \tau_0 < T_c$. And finally, the system performance reaches a constant value for completely decorrelated fields, *i.e.* $\tau_0 > T_c$, labeled zone III. The reasons behind these behaviors are explained in Section 3.2. These curves furthermore prove that the BER improves as the OFDM symbol period decreases. It may be explained by noting that phase noise compensation is similar to a high-pass filter with a cutoff frequency equal to the OFDM symbol period [21,22]. For a shorter OFDM symbol period, the residual phase noise is therefore reduced as noted in [56] for uncorrelated fields.

Moreover, in Fig. 3(a), the dash–dot curve represents the theoretical approximation of the system performance in terms of the time delay if the phase noise is not mitigated. According to Eq. (9), the BER deteriorates as the time delay increases until it remains

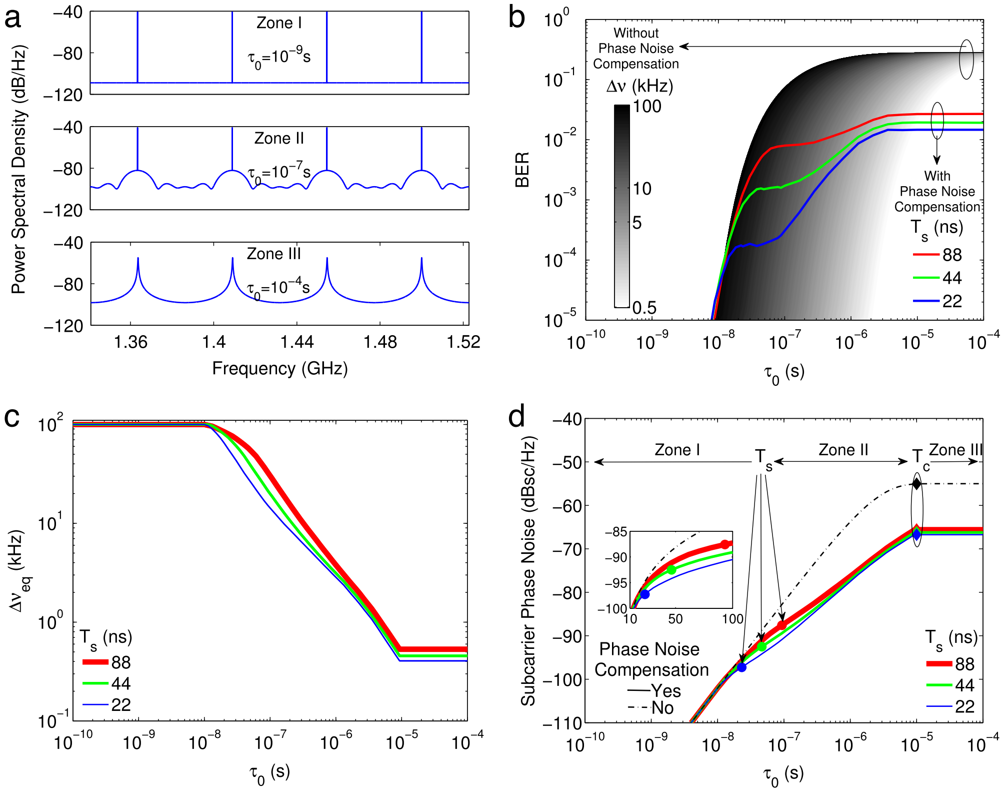

Fig. 4. System performance where a laser linewidth of 100 kHz is used and the AWGN is excluded. (a) Spectral samples in each zone for an unmodulated OFDM symbol period of 22 ns. The pilot amplitude is set to unit and the data subcarriers have been zeroed. (b) BER as a function of the time delay without (black curves) and with (color curves) phase noise mitigation. Former curves have the laser linewidth as a parameter while the OFDM symbol period is the parameter for latter curves. (c) Equivalent laser linewidth vs. time delay with the OFDM symbol period as parameter. (d) Subcarrier phase noise in terms of the time delay in the absence (dash–dot curve) and in the presence (solid curves) of pilot-assisted phase-noise estimation, 10 kHz is the selected offset frequency. For solid curves, the OFDM symbol period is the parameter. (For interpretation of the references to color in this figure legend, the reader is referred to the web version of this article.)

constant for completely decorrelated fields. This behavior makes sense since in the third zone, both lasers become uncorrelated [38,42] and the system degradation then reaches its maximum value [22]. It is worth noting here that the theoretical BER is independent of the OFDM symbol period. We can finally observe in Fig. 3(a) how the system performance improves by the use of pilot-assisted equalization in terms of the time delay. For small time delays, however, it is negligible owing to the high phase-correlation degree between the fields. In zone II, this improvement reaches its maximum value, and for time delays greater than the coherence time, the phase noise reduction remains constant. These improvements are further illustrated by constellations in Fig. 3(a.i–iii). At the same time, constellations show that phase noise reduction diminishes CPE and the residual phase noise is mainly because of ICI [23,24].

In order to verify the existence of the three zones and to discard the possibility of an effect associated to the error-counting method, we find the EVM. Solid curves of Fig. 3(b) show the EVM as a function of the time delay when pilot-assisted equalization is taken into account. As with the BER, the EVM exhibits the same three zones with the same two boundaries, at the OFDM symbol period and at the coherence time. As mentioned above, during OFDM symbol transmission, pilots are uniformly inserted into the OFDM symbol for channel estimating purposes. In RoF systems, nevertheless, the ideal CPE compensation [30] could be realized as long as the wireless channel is not frequency selectivity. In this scenario through dashed curves, the EVM as the fields become decorrelated is also depicted in Fig. 3(b). Once again, the three regimes are appreciated following similar characteristics, for instance, the EVM slowly deteriorates in the zone II. All this means that the BER behavior is hence due to the phase noise is diminished as can be seen when comparing theoretical and simulation results. Of course, the system performance improves substituting the pilot-assisted equalization via CPE compensation to combat the phase noise. Fig. 3(b.i) demonstrates the previous statement, namely, CPE mitigation outperforms pilot-aided phase-noise correction in terms of estimating phase noise.

3.2. Power spectral density and subcarrier phase noise

The result of Fig. 3(a), namely, that the BER exhibits three performance regimes as the time delay increases when pilot-assisted phase-noise estimation is employed, can be explained by two approaches.

Firstly, via both the PSD profile of the received OFDM unmodulated carriers, which is calculated in Appendix, and the effectiveness of the phase noise compensator. According to an OFDM symbol period of 22 ns, Fig. 4(a) represents these PSDs in each of the three zones. It has a different profile in each one. The PSD for small time delays is characterized by Dirac delta functions, whose amplitude depends on the time delay. In the second zone, a sinc shape, with spectral zeros separated by the reciprocal of the time delay, is superimposed to the deltas. And finally, for a time delay greater than the coherence time, a PSD with a Lorentzian profile is revealed whose linewidth is equal to two times the laser linewidth. The PSD behavior then indicates how ICI appears and evolves through the transitions from zone I to II and from zone II to III, and by the effectiveness of the phase noise compensator, which diminishes CPE, the system behavior makes sense.

To quantify this qualitative result, the subcarrier phase noise was previously introduced. Since the performance of uncompensated does not depends on the OFDM symbol period, see Eq. (A.5),

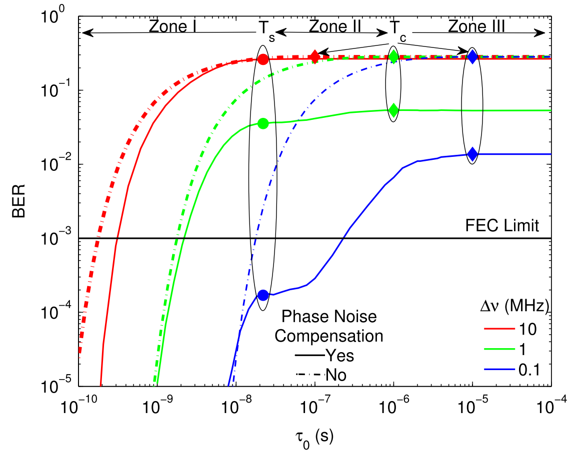

Fig. 5. BER as a function of the time delay with the laser linewidth as parameter and without AWGN. The dash–dot and solid curves are without and with pilot-assisted equalization, respectively. For solid curves, the OFDM symbol period is equal to 22 ns.

we find the equivalent laser linewidth, $\Delta\nu_{eq}$, through Fig. 4(b). This figure depicts the BER as a function of the time delay without (gray contour curves whose parameter is the laser linewidth) and with (color curves whose parameter is the OFDM symbol period) phase noise mitigation. In zone I and II, we find the equivalent laser linewidth by calculating the intersection between these curves, whereas for completely phase-decorrelated fields, the equivalent laser linewidth evidently remains the same. The resulting equivalent laser linewidth against the amount of phase-correlation between the fields is plotted in Fig. 4(c). Fig. 4(d) shows thus the subcarrier phase noise in terms of the time delay in the absence (dash–dot curve) and in the presence (solid curves) of pilot-assisted equalization. This figure explains quantitatively the results of Fig. 3(a), namely, the differences (or boundaries) between zones I, II, and III appears as long as the pilot-assisted equalization is employed.

3.3. Laser phase noise and AWGN effects

In this Section, we initially study the system performance dependence on laser linewidth. Fig. 5 presents the BER as a function of the time delay with the laser linewidth as parameter. Once again, dash–dot curves are obtained from the theoretical approximation of Eq. (9) and solid curves represent the simulation results with phase noise mitigation. We selected an OFDM symbol period of 22 ns corresponding to 10-Gb/s bit rate. Several observations can be highlighted. First of all, the BER reaches its maximum value when the fields are completely decorrelated. Notice that all three theoretical curves converge to the same value above this instant [22]. As for the simulation results, the BER improvement is highly dependent on laser linewidth. This improvement increases as the laser phase noise is reduced [38]. Evidently, by increasing the laser linewidth, the coherence time is reduced and when it approaches the OFDM symbol period, no improvement can be obtained by the use of the phase noise compensator. The zone II then disappears as the coherence time gets closer to the OFDM symbol period. This is observed on the red solid curve for a laser with a 10-MHz linewidth.

The above results can obviously never correspond to experimental observations because AWGN is yet to be included. We therefore repeated our simulations including the SNR. The results are depicted in Fig. 6. The maximum admissible time delay is easily identified and clearly decreases when increasing the laser phase noise and/or AWGN. For example, if a given application imposes a time delay of 1 ns, a laser with a linewidth less than 1 MHz and at least an SNR of 24 dB are required in order to reach the FEC limit. Notice finally that for a SNR above 30 dB, the influence of AWGN is negligible compared to phase noise. The first, second, and third zones so persist for SNRs greater than 30 dB, but as the AWGN becomes more dominant, these will be less apparent.

4. Discussion of results

According to the system model, the current results can be applied to the study and design of most popular RoF-OFDM systems. It suffices to select the appropriate combination of our system parameters: time delay, laser linewidth, SNR, OFDM parameters, mm-wave frequency, among others. In this section, we discuss the transmission distance limits imposed by not only fiber loss but also fiber dispersion that satisfy the FEC limit requirement. The loss limit results from the ratio between the available channel loss and fiber loss [43]. The dispersion limit depends on the time delay, which in turn may be decomposed into a delay, τ_0^{tech}, associated to the optical up-conversion technique and another delay, τ_0^{fiber}, due to fiber dispersion, namely $\tau_0 = \tau_0^{tech} + \tau_0^{fiber}$ [38,57]. In the following, we focus on OFDM-based RoF systems with perfectly phase-correlated optical tones at the central station, *i.e.* $\tau_0^{tech} = 0$ s. These systems correspond to the solution of creating low phase noise mm-wave signals and may be implemented through various generation techniques based on optical up-conversion, such as externally modulated laser, multimode light sources, and heterodyning two lasers [6,9–11]. The time delay is hence only a consequence of the fiber dispersion, *i.e.* $\tau_0 = \tau_0^{fiber}$. For an OFDM signal in the presence of a separation between subcarriers much less than the RF, it results in [41,43]:

$$\tau_0 = D \cdot L \cdot \frac{\lambda^2}{c} \cdot f_{RF}, \tag{13}$$

where $D = 18$ ps/(nm–km) is the dispersion parameter in standard single mode fibers, L is the fiber length, $\lambda = 1550$ nm is the laser wavelength, and $c = 3 \times 10^8$ m/s is the speed of light in vacuum. Fig. 7 displays the loss and dispersion limitation on the fiber length in terms of the laser linewidth. The available channel loss and fiber loss were fixed at 20 dB and 0.18 dB/km, respectively. The dispersion-limited curves were obtained via both simulations taking into account a SNR of 24 dB and Eq. (13). For each laser linewidth, the time delay given by Eq. (13) was determined from Fig. 5 at the adopted BER threshold. The mm-wave frequency parameter extends from 30 to 110 GHz. This figure reveals that the transmission distance is loss-limited for narrow laser linewidths and dispersion-limited for lasers with a broad linewidth. The intersection between the loss and dispersion limits depends on the mm-wave frequency. For a range from 30 to 110 GHz, the laser linewidth at the intersection decreases from 2.5 to 0.55 MHz. Nevertheless, the dispersion limit imposed by the phase decorrelation induced by chromatic dispersion on the two beating signals separated by f_{RF} could be relaxed at the cost of increasing the RoF system complexity. In this regard, some possible alternatives are exclusive time delay precompensations for the different optical lengths between the single central station and the numerous base stations [36,37], and sophisticated phase noise reduction techniques at the mobile terminals, such as post phase noise suppression algorithm and RF-pilot phase noise mitigation [41]. As mentioned before, we should note that pilot-assisted equalization does not demand any additional requirement since it possesses the purpose of estimating the wireless channel [23,24]. To conclude, for the simulated laser linewidths, the maximum transmission distance lies in the first zone. As consequence, in practical scenarios, the BER would rapidly deteriorate as the fields become decorrelated. If the laser linewidth is less than 100 kHz, the FEC limit lies in zone II.

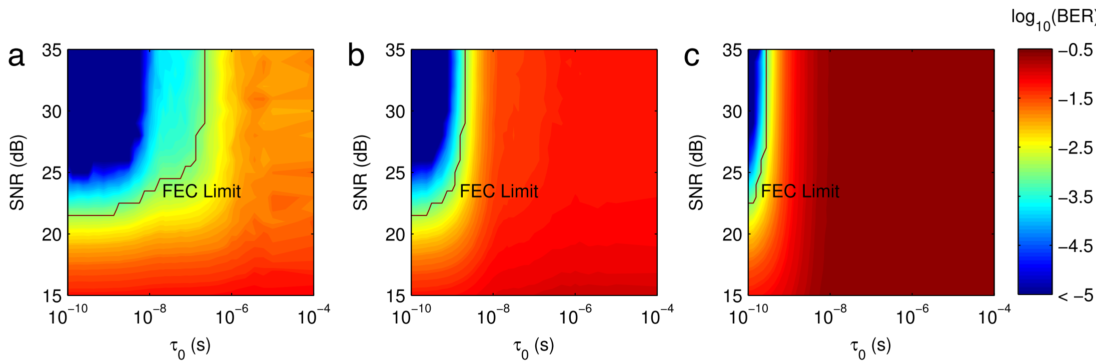

Fig. 6. BER in terms of the time delay and SNR for (a) 100 kHz, (b) 1 MHz, and (c) 10-MHz laser linewidths in the presence of the phase noise compensator. An OFDM signal with a symbol period of 22 ns was used.

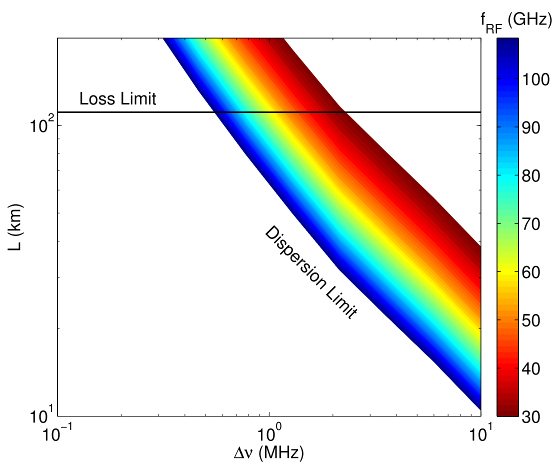

Fig. 7. Transmission distance limits as a function of laser linewidth.

5. Conclusion

We perform extensive simulations and theoretical analysis to evaluate the impact of different phase decorrelation degrees on the performance of RoF-OFDM systems with pilot-aided equalization, finding for the first time three different regimes. The first boundary of these regimes lies at a time delay equal to the OFDM symbol period and the second one, at a time delay equal to the coherence time. To explain this behavior, we first studied the received PSD and we showed that the profile in each zone greatly varies. In particular, ICI becomes appreciable in zones II and III, and since our equalizer only diminishes CPE, it is clear that the effectiveness of the phase noise compensator will create the three performance regimes. To further gain insight on the explanation behind the three zones, the subcarrier phase noise with and without pilot-assisted phase-noise estimation was presented, appreciating again the three performance zones in the presence of pilot-aided equalization. Additionally, we noticed how the EVM is affected by the correlation degree when the ideal CPE compensation instead of pilot-aided equalization is employed. The system performance also exposes similar characteristics with the same two boundaries, for example, a fast degradation of the system as long as the time delay does not exceed the OFM symbol period. All this implies that the system performance is a direct consequence of the phase noise mitigation. After that we proceeded to study the laser linewidth influence on the BER. As expected, system performance deteriorates by increasing the linewidth, and as the coherence time becomes closer to the symbol period, the second zone disappears. The influence of AWGN was also evaluated. We found that it is negligible compared to laser phase noise for a SNR greater than 30 dB. Finally, we calculated the maximum range of the RoF optical segment for optical up-conversion techniques employing phase-correlated fields at the transmitter, which can be used by designers to dimension their network. The fiber length is loss-limited up to about 1 MHz laser linewidth, after which it becomes dispersion-limited. We believe our results will have an impact in RoF system design, so partial decorrelation should be taken in account.

Appendix

The transmitted OFDM signal filled with unit-amplitude pilots is represented as:

$$s_p(t) = \sum_{l=0}^{N_{sc}-1} \exp(j2\pi f_l t), \tag{A.1}$$

with $f_l = l/T_s$ representing the lth frequency subcarrier. Inserting Eq. (14) in Eq. (8) without AWGN, the received OFDM signal acquires the form of:

$$r_p(t) = \sum_{l=0}^{N_{sc}} \exp(j2\pi f_l t)\ \exp[j\Delta\phi(t, \tau_0)]. \tag{A.2}$$

By using the Wiener–Khintchine theorem, its PSD can be obtained:

$$S_{r_p}(f) = \sum_{l=0}^{N_{sc}} \delta(f - f_l) * \mathcal{F}\Big\{\langle \exp\{j[\Delta\phi(t, \tau_0) - \Delta\phi(t+\tau, \tau_0)]\}\rangle\Big\}, \tag{A.3}$$

where $*$ means the convolution operation. Based on results reported in [38,42], it results in:

$$S_{r_p}(f) = \sum_{l=0}^{N_{sc}} \Bigg\{ \frac{\Delta\nu}{\pi[\Delta\nu^2 + (f - f_l)^2]} \times \left\{ 1 - \exp(-2\pi\Delta\nu\tau_0) \left[1 + \left(\frac{\Delta\nu}{f - f_l}\right)^2 \right]^{1/2} \times \cos\left[2\pi(f - f_l)\tau_0 - \tan^{-1}\left(\frac{\Delta\nu}{f - f_l}\right) \right] \right\} + \exp(-2\pi\Delta\nu\tau_0)\,\delta(f - f_l) \Bigg\}. \tag{A.4}$$

We finally determine the PSD at an offset frequency, Δf, from a single subcarrier by:

$$S_{r_p}(f_l+\Delta f) = \frac{\Delta\nu}{\pi(\Delta\nu^2+\Delta f^2)}\left\{1-\exp(-2\pi\,\Delta\nu\tau_0)\left[1+\left(\frac{\Delta\nu}{\Delta f}\right)^2\right]^{1/2} \times \cos\left[2\pi\,\Delta f\,\tau_0-\tan^{-1}\left(\frac{\Delta\nu}{\Delta f}\right)\right]\right\}. \tag{A.5}$$

References

[1] C. Lim, A. Nirmalathas, M. Bakaul, P. Gamage, K.-L. Lee, Y. Yang, D. Novak, R. Waterhouse, Fiber-wireless networks and subsystem technologies, J. Light. Technol. 28 (4) (2010) 390–405.

[2] M. Cudak, A. Ghosh, T. Kovarik, R. Ratasuk, T.A. Thomas, F.W. Vook, P. Moorut, Moving towards mmWave-based beyond-4G (B-4G) technology, in: IEEE 77th Vehicular Technology Conference (VTC Spring), 2013, pp. 1–5.

[3] W. Alliance, Defining the future of multi-gigabit wireless communications, WiGig White Paper, 2010.

[4] P. Wang, Y. Li, L. Song, B. Vucetic, Multi-gigabit millimeter wave wireless communications for 5G: From fixed access to cellular networks, IEEE Commun. Mag. 53 (1) (2015) 168–178.

[5] FCC, Wireless telecommunications bureau seeks comment on requests of zenfi networks, Inc. and Geneva communications LLC for waiver to authorize service in the 102-109.5 GHz band, Public Note, 2015.

[6] J. Beas, G. Castanon, I. Aldaya, A. Aragón-Zavala, G. Campuzano, Millimeter-wave frequency radio over fiber systems: A survey, IEEE Commun. Surv. Tutor. 15 (4) (2013) 1593–1619.

[7] Z. Jia, J. Yu, G. Ellinas, G.-K. Chang, Key enabling technologies for optical–wireless networks: Optical millimeter-wave generation, wavelength reuse, and architecture, J. Light. Technol. 25 (11) (2007) 3452–3471.

[8] V. Thomas, M. El-Hajjar, L. Hanzo, Millimeter-wave radio over fiber optical upconversion techniques relying on link non-linearity, IEEE Commun. Surv. Tutor. (2015).

[9] T. Sakamoto, T. Kawanishi, M. Izutsu, 19 × 10 GHz electro-optic ultra-flat frequency comb generation only using single conventional Mach–Zehnder modulator, in: Conference on Lasers and Electro-Optics and Quantum Electronics and Laser Science Conference, 2006, pp. 1–2.

[10] P.M. Anandarajah, et al., Generation of coherent multicarrier signals by gain switching of discrete mode lasers, IEEE Photonics J. 3 (1) (2011) 112–122.

[11] F. Brendel, et al., Chromatic dispersion in 60 GHz radio-over-fiber networks based on mode-locked lasers, J. Light. Technol. 29 (24) (2011) 3810–3816.

[12] V. Thomas, M. El-Hajjar, L. Hanzo, Performance improvement and cost reduction techniques for radio over fiber communications, IEEE Commun. Surv. Tutor. 17 (2) (2015) 627–670.

[13] J. Armstrong, OFDM for optical communications, J. Light. Technol. 27 (3) (2009) 189–204.

[14] N. Cvijetic, OFDM for next-generation optical access networks, J. Light. Technol. 30 (4) (2012) 384–398.

[15] W. Shieh, I. Djordjevic, Orthogonal Frequency Division Multiplexing for Optical Communications, Academic Press, 2010.

[16] H. Lin, Flexible configured OFDM for 5G air interface, IEEE Access 3 (2015) 1861–1870.

[17] Y. Wu, H. Luo, M. Ding, R. Liu, A high performance frequency offset estimator for OFDM systems based on a special preamble, in: IEEE 17th International Symposium on Personal, Indoor and Mobile Radio Communications, 2006, pp. 1–4.

[18] P. Malarvezhi, R. Kumar, A modified preamble structure based carrier frequency offset (CFO) compensation in an OFDM system, in: International Conference on Communications and Signal Processing (ICCSP), 2013, pp. 504–508.

[19] T. Maeda, N. Matsuno, S. Hori, T. Yamase, T. Tokairin, K. Yanagisawa, H. Yano, R. Walkington, K. Numata, N. Yoshida, A low-power dual-band triple-mode WLAN CMOS transceiver, IEEE J. Solid-State Circuits 41 (11) (2006) 2481–2490.

[20] L. Tomba, On the effect of Wiener phase noise in OFDM systems, IEEE Trans. Commun. 46 (5) (1998) 580–583.

[21] J. Stott, The effects of phase noise in COFDM, EBU Technical Review, 1998, pp. 12–25.

[22] A.G. Armada, Understanding the effects of phase noise in orthogonal frequency division multiplexing (OFDM), IEEE Trans. Broadcast. 47 (2) (2001) 153–159.

[23] S. Wu, Y. Bar-Ness, OFDM systems in the presence of phase noise: Consequences and solutions, IEEE Trans. Commun. 52 (11) (2004) 1988–1996.

[24] Q. Zou, A. Tarighat, A.H. Sayed, Compensation of phase noise in OFDM wireless systems, IEEE Trans. Signal Process. 55 (11) (2007) 5407–5424.

[25] T. Hwang, C. Yang, G. Wu, S. Li, G.Y. Li, OFDM and its wireless applications: A survey, IEEE Trans. Veh. Technol. 58 (4) (2009) 1673–1694.

[26] A.G. Armada, M.C. Ramón, Rapid prototyping of a test modem for terrestrial broadcasting of digital television, IEEE Trans. Consumer Electron. 43 (4) (1997) 1100–1109.

[27] X. Yi, W. Shieh, Y. Ma, Phase noise effects on high spectral efficiency coherent optical OFDM transmission, J. Light. Technol. 26 (10) (2008) 1309–1316.

[28] W.-R. Peng, Analysis of laser phase noise effect in direct-detection optical OFDM transmission, J. Light. Technol. 28 (17) (2010) 2526–2536.

[29] C.-C. Wei, J. Chen, Study on dispersion-induced phase noise in an optical OFDM radio-over-fiber system at 60 GHz band, Opt. Express 18 (20) (2010) 20774–20785.

[30] X. Yi, W. Shieh, Y. Tang, Phase estimation for coherent optical OFDM, IEEE Photonics Technol. Lett. 19 (9/12) (2007) 919.

[31] S.L. Jansen, I. Morita, T.C.W. Schenk, N. Takeda, H. Tanaka, Coherent optical 25.8 Gb/s OFDM transmission over 4160 km SSMF, J. Light. Technol. 26 (1) (2008) 6–15.

[32] S. Randel, S. Adhikari, S.L. Jansen, Analysis of RF-pilot-based phase noise compensation for coherent optical OFDM systems, IEEE Photonics Technol. Lett. 22 (17) (2010) 1288–1290.

[33] S. Cao, P.Y. Kam, C. Yu, pilot-aided Decision-aided, decision-feedback phase estimation for coherent optical OFDM systems, IEEE Photonics Technol. Lett. 24 (22) (2012) 2067–2069.

[34] X. Escayola, I. Cano, M. Santos, J. Prat, Laser linewidth requirements for remote heterodyne OFDM based PON scenario, in: 16th International Conference on Transparent Optical Networks (ICTON), 2014, pp. 1–4.

[35] Q. Fan, J. He, M. Chen, J. Liu, L. Chen, Low-complexity phase noise compensation approach for co-ofdm systems, IEEE Photonics Technol. Lett. (99) (2016). 1–1.

[36] T. Shao, E. Martin, P.M. Anandarajah, C. Browning, V. Vujicic, R. Llorente, L.P. Barry, Chromatic dispersion-induced optical phase decorrelation in a 60 GHz OFDM-RoF system, IEEE Photonics Technol. Lett. 26 (20) (2014) 2016–2019.

[37] E.P. Martin, et al., 25 Gb/s OFDM 60-GHz radio over fiber system based on a gain switched laser, J. Light. Technol. 33 (8) (2015) 1635–1643.

[38] U. Gliese, S. Norskov, T. Nielsen, Chromatic dispersion in fiber-optic microwave and millimeter-wave links, IEEE Trans. Microw. Theory Tech. 44 (10) (1996) 1716–1724.

[39] P. Gallion, G. Debarge, Quantum phase noise and field correlation in single frequency semiconductor laser systems, IEEE J. Quantum Electron. 20 (4) (1984) 343–349.

[40] R. Tkach, A. Chraplyvy, Phase noise and linewidth in an InGaAsP DFB laser, J. Light. Technol. 4 (11) (1986) 1711–1716.

[41] C.-C. Wei, C.-T. Lin, H.-T. Huang, W.-L. Liang, S. Chi, Estimation and suppression of dispersion-induced phase noise in W-band direct-detection OFDM radio-over-fiber systems, J. Light. Technol. 32 (20) (2014) 3874–3884.

[42] P. Gallion, F. Mendieta, R. Leconte, Single-frequency laser phase-noise limitation in single-mode optical-fiber coherent-detection systems with correlated fields, J. Opt. Soc. Am. 72 (9) (1982) 1167–1170.

[43] G.P. Agrawal, Fiber-Optic Communication Systems, John Wiley & Sons, 2012.

[44] P. Rabiei, W. Namgoong, N. Al-Dhahir, Pilot design for OFDM systems in the presence of phase noise, in: Conference Record of the Forty Fourth ASILOMAR Conference on Signals, Systems and Computers, 2010, pp. 516–520.

[45] L. Hanzo, M. Münster, B. Choi, T. Keller, OFDM and MC-CDMA for Broadband Multi-user Communications, WLANs and Broadcasting, John Wiley & Sons, 2005.

[46] R.A. Shafik, M.S. Rahman A.R, Islam On the extended relationships among EVM, BER and SNR as performance metrics, in: International Conference on Electrical and Computer Engineering, 2016, pp. 408–411.

[47] A. Georgiadis, Gain, phase imbalance, and phase noise effects on error vector magnitude, IEEE Trans. Veh. Technol. 53 (2) (2004) 443–449.

[48] M. Seimetz, High-Order Modulation for Optical Fiber Transmission, Springer, 2009.

[49] D.A. Guimaraes, Digital Transmission: A Simulation-Aided Introduction with VisSim/Comm, Springer Science & Business Media, 2010.

[50] A. Tychopoulos, O. Koufopavlou, I. Tomkos, FEC in optical communications - A tutorial overview on the evolution of architectures and the future prospects of outband and inband FEC for optical communications, IEEE Circuits Devices 22 (6) (2006) 79–86.

[51] M.D. McKinley, K.A. Remley, M. Myslinski, J.S. Kenney, D. Schreurs, B. Nauwelaers, EVM calculation for broadband modulated signals, in: Conference of the 64th ARFTG, 2004, pp. 45–52.

[52] IEEE standard for telecommunications and information exchange between systems - LAN/MAN specific requirements - Part 11: Wireless medium access control MAC and physical layer PHY specifications: High speed physical layer in the 5 GHz band, 1999, iEEE Std 802.11a-1999, 1999, pp. 1–102.

[53] H. Packard, RF microwave phase noise measurement seminar, 1988.

[54] W.J. Riley, Handbook of frequency stability analysis. US Department of Commerce, National Institute of Standards and Technology Gaithersburg, MD, 2008.
[55] D. Petrovic, W. Rave, G. Fettweis, Effects of phase noise on OFDM systems with and without PLL: Characterization and compensation, IEEE Trans. Commun. 55 (8) (2007) 1607–1616.
[56] V. Syrjala, M. Valkama, N.N. Tchamov, J. Rinne, Phase noise modelling and mitigation techniques in OFDM communications systems, in: Wireless Telecommunications Symposium, 2009, pp. 1–7.
[57] R.-P. Braun, Tutorial: Fiber radio systems, applications and devices, in: 24th European Conference on Optical Communication, vol. 2, 1998, pp. 87–119.

David Zabala-Blanco received the B.S. degree in electronic systems engineering from Escuela Militar de Ingenieria, La Paz, Bolivia, in 2011 and the MSc degree in electronic engineering from Tecnologico de Monterrey, Monterrey, Mexico in 2014. He is currently pursuing the Ph.D. degree in information and communications technology at Tecnologico de Monterrey. His research interest includes the carrier frequency offset effect in OFDM performance and millimeter-wave radio-over-fiber systems.

Gabriel Campuzano is an associate professor at the Department of Electrical and Computational Engineering at Tecnologico de Monterrey since august 2003. He received his undergraduate degree as an Industrial Physics Engineer from the same University (Tecnologico de Monterrey), Campus Monterrey, and holds a MSc (DEA) in Microwaves and Optoelectronics from the Universite de Pierre et Marie Curie, France. He then received the Ph.D. degree in Optical Communications from the Ecole Nationale Superieure des Telecommunications (Telecom Paris-Tech), France. His fields of interest range in Radio over Fiber Systems for wireless access networks, including mobility in picocells, novel optoelectronic functions, and quantum cryptographic systems for telecommunication wavelengths.

Ivan Aldaya received the B.E. in telecommunication engineering from the Public University of Navarre (UPNA), Pamplona, in 2005 and a PhD in Communications and Information Technologies from the Monterrey Institute of Technology and Higher Education (ITESM) in 2013. He holds a postdoc with the Optical Communications Research group at ITESM and a second postdoc at the Laboratory of Optical Communication within the Physics Institute at the State University of Campinas (UNICAMP). He is currently assistant professor at the State University of Sao Paulo (UNESP). His main research interests include compensation of nonlinear distortion, optical injection locking, and integrated photonics.

Gerardo Castañón is received the Bachelor of Science in Physics Engineering from Tecnologico de Monterrey (ITESM), Mexico in 1987. He received the Master of Science degree in Physics (Optics) from the Ensenada Research Centre and Higher Education, Mexico in 1989. He received the Master of Science degree in Electronics Engineering from ITESM in 1990. He also received the Master and Ph.D. degrees in Electrical and Computer Engineering from the State University of New York (SUNY) at Buffalo in 1995 and 1997 respectively. He is actually working in the Department of Electrical and Computer Engineering at ITESM since September of 2002. Dr. Castañón has over 60 publications in journals, book chapters and conferences and 4 international patents.

César Vargas-Rosales has a Ph.D. and a Master of Science degrees in Electrical Engineering from Louisiana State University in Communications and Signal Processing (1992, 1996). He is a member of the Mexican National Researchers System (SNI), the Mexican Academy of Engineering (AIM), and the Mexican Academy of Science (AMC). He was also the Technical Program Chair of the IEEE Wireless Communications and Networking Conference (IEEE WCNC 2011). He is the co-author of the book Position Location Techniques and Applications (Academic Press). Currently, he is with the School of Engineering and Sciences at Tecnologico de Monterrey.